during the second stage of reduction represents adjustments of the surrounding protein necessary to accommodate a longer Fe1-Fe2 distance. We note that difference electron density maps show a longer Fe1-Fe2 distance in deoxy- than in metHr.[8] This proposal is consistent with our earlier suggestion[7] that alteration of the net charge on the binuclear cluster requires adjustments by the surrounding protein.

The third stage, labeled k_3 in Scheme I, is proposed to be the transformation of met′ to met, after which "normal" reduction kinetics resume. The exact nature of the difference between met and met′ is unclear. The preceding discussion suggests a longer Fe1-Fe2 distance in met′ than in met. Another possibility is that met′ has the sixth coordination position on Fe2 occupied by OH^-. Occupancy of this coordination site in met′ would explain the inability of N_3^- to significantly perturb the absorption spectrum of the second-stage product. The rate-determining step for the third stage would then be dissociation of OH^- from Fe2. This proposal is consistent with the kinetics of reduction of the anion adducts, metHrX. Reductions of metHrX are uniphasic, with the rate-determining step being dissociation of X^-.[43] Also, the rate of reduction of metHrOH has been reported to be dependent on conversion to metHr.[44]

Our scheme unifies the kinetics of reduction of octameric Hrs from *T. zostericola* and *P. gouldii* and in addition satisfactorily explains many chemical and physical properties of these two proteins determined in this study as well as in many previous studies. We note that monomeric metmyoHr from *T. zostericola* has reduction kinetics based on absorbance changes, which are quite similar to those of the octameric Hrs.[45] A scheme somewhat different from Scheme I was proposed to explain the kinetics for myoHr, but on the basis of available data, Scheme I seems equally applicable.[46] The apparent physiological reducing agent for metHr, namely, cytochrome b_5,[18] is an "outer-sphere" reagent, and, therefore, is also expected to function according to Scheme I. The implications of our results for the reduction of metHr in vivo will be discussed elsewhere.[47]

Acknowledgment. This work has been supported by grants from the National Institutes of Health (D.M.K., GM 37851; P.G.D., GM 16406).

(43) Olivas, E.; deWaal, J. A.; Wilkins, R. G. *J. Inorg. Biochem.* **1979**, *11*, 205-212.

(44) Bradič, Z.; Wilkins, R. G. *Biochemistry* **1983**, *22*, 5396-5401.

(45) Armstrong, G. D.; Sykes, A. G. *Inorg. Chem.* **1986**, *25*, 3725-3729.

(46) From comparisons of the published absorption spectral time courses,[13,45] it appears that, for myoHr, direct reduction competes relatively effectively with disproportionation during the second stage.

(47) Utecht, R. E.; Kurtz, D. M., Jr., submitted for publication in *Biochim. Biophys. Acta.*

Crown Ether-Cation Decomplexation Mechanics. ^{23}Na NMR Studies of the Sodium Cation Complexes with Dibenzo-24-crown-8 and Dibenzo-18-crown-6 in Nitromethane and Acetonitrile

Alfred Delville,† Harald D. H. Stöver, and Christian Detellier*

Contribution from the Ottawa-Carleton Chemistry Institute, Ottawa University Campus, Ottawa, Ontario K1N 9B4, Canada. *Received February 17, 1987*

Abstract: The mechanisms and the activation parameters of decomplexation have been determined by ^{23}Na NMR for dibenzo-24-crown-8 (DB24C8)-$NaPF_6$ in nitromethane, dibenzo-18-crown-6 (DB18C6)-NaX in acetonitrile (X = BF_4^-, BPh_4^-), and DB18C6-NaY in nitromethane (Y = PF_6^-, BPh_4^-). For DB24C8-$NaPF_6$ in nitromethane, the decomplexation follows a bimolecular exchange mechanism for $[Na^+]_T > 2 \times 10^{-3}$ M, characterized by $\Delta H^\ddagger = 30 \pm 2$ kJ mol^{-1} and $\Delta S^\ddagger = -37 \pm 10$ J mol^{-1} K^{-1}. At lower sodium concentrations, the mechanism is predominantly unimolecular with $\Delta G^\ddagger_{300} \sim 63$ kJ mol^{-1}. For Na^+-DB18C6 in acetonitrile, the mechanism is purely unimolecular with $\Delta H^\ddagger = 40 \pm 2$ kJ mol^{-1} and $\Delta S^\ddagger = -44 \pm 8$ J mol^{-1} K^{-1}. In nitromethane, the bimolecular exchange mechanism is in competition with the unimolecular one. The contributions of the two mechanisms have been separated from the observed rate constants: at 300 K, $\Delta G^\ddagger_{bi} = 48 \pm 4$ kJ mol^{-1} and $\Delta G^\ddagger_{uni} = 60 \pm 3$ kJ mol^{-1}. The activation parameters have been determined for the unimolecular decomplexation mechanism: $\Delta H^\ddagger = 37 \pm 3$ kJ mol^{-1} and $\Delta S^\ddagger = -78 \pm 8$ J mol^{-1} K^{-1}. The comparison with literature data showed that the unimolecular decomplexation mechanism is favored in high-donicity solvents, despite a higher activation enthalpy, which is compensated by a higher activation entropy. It is suggested that the unimolecular decomplexation of Na^+-DB18C6 involves a desolvation step accompanying conformational changes.

Molecular recognition phenomena are being studied at higher and higher levels of complexity. The design of host molecules incorporating specific characteristics has led to high discrimination between guest molecules or cations for the formation of the "host-guest" complex. The crown ethers (chorands, coronands), first synthesized by Pedersen in 1967,[1] opened the way to the cryptands,[2] the spherands,[3] the lariat crown ethers,[4] and channel assemblies.[5] However, the increased sophistication of the relationship between host structure and host-guest complexation lies on mechanisms of complexation-decomplexation which are still poorly understood. This is the case even for basic systems such as the simple coronands. In fact, the crown ether, the cation, the

† Chargé de Recherches FNRS. Permanent address: Institut de Chimie Organique et de Biochimie B6, Université de Liège au Sart-Tilman, B-4000, Liège, Belgium.

(1) Pedersen, C. J. *J. Am. Chem. Soc.* **1967**, *89*, 7017-7036.

(2) Lehn, J. M. *Acc. Chem. Res.* **1978**, *11*, 49-57.

(3) Cram, D. J.; Kaneda, T.; Helgeson, R. C.; Brown, S. B.; Knobler, C. B.; Maverick, E.; Trueblood, K. N. *J. Am. Chem. Soc.* **1985**, *107*, 3645-3657.

(4) Schultz, R. A.; White, B. D.; Dishong, D. M.; Arnold, K. A.; Gokel, G. W. *J. Am. Chem. Soc.* **1985**, *107*, 6659-6668.

(5) (a) Walba, D. M.; Richards, R. M.; Sherwood, S. P.; Haltiwanger, R. C. *J. Am. Chem. Soc.* **1981**, *103*, 6213-6215. (b) Van Beijnen, A. J. M.; Nolte, R. J. M.; Zwikker, J. W.; Drenth, W.; *Recl.: J. R. Neth. Chem. Soc.* **1982**, *101*, 409-410.

0002-7863/87/1509-7293$01.50/0

associated anion, and the solvent molecules form a complex supramolecular assembly in which each partner plays a role in the whole reorganization which accompanies the cation capture or escape.

Of particular interest is the characterization of the mechanism by which the complexing agent exchanges host alkali metal cations. It has been shown that the complexation follows a multistep mechanism, in which either removal of the solvent or ligand rearrangement may become rate determining.[6-8] Alkali metal cation NMR is a very efficient tool for the study of the decomplexation kinetics.[9] ^{7}Li,[10] ^{23}Na,[11-21] ^{39}K,[22,23] and ^{133}Cs[24-27] have been used for this purpose. So far, unimolecular decomplexation and bimolecular cation interchange have been the two most considered mechanisms.[11] The unimolecular decomplexation (dissociative mechanism) has been found to be the most common. However, a competition between these two mechanisms was observed in the case of sodium tetraphenylborate complexed by DB24C8 in nitromethane,[12] the exchange being predominantly bimolecular for higher sodium concentrations and predominantly unimolecular for the lower ones. A bimolecular exchange mechanism was also found to be efficient for K^+–18C6 in several nonaqueous solvents[22] and for Cs^+–DB21C7 and Cs^+–DB24C8 in methanol and acetone,[27] while for Na^+–18C6, the exchange was unimolecular (dissociative) in methanol and bimolecular in propylene carbonate.[13] The role of the anion has also been investigated by Popov and co-workers,[14,15] who have shown that the thiocyanate anion favors the bimolecular mechanism, whereas the dissociative mechanism is predominant in the case of tetraphenylborate.[14]

In this paper we describe three sodium–crown complexes that are characterized by different decomplexation mechanisms: unimolecular dissociative in the case of DB18C6 in acetonitrile, bimolecular cation interchange in the case of DB24C8 in nitromethane, and a competition between these two mechanisms in the case of DB18C6 in nitromethane.

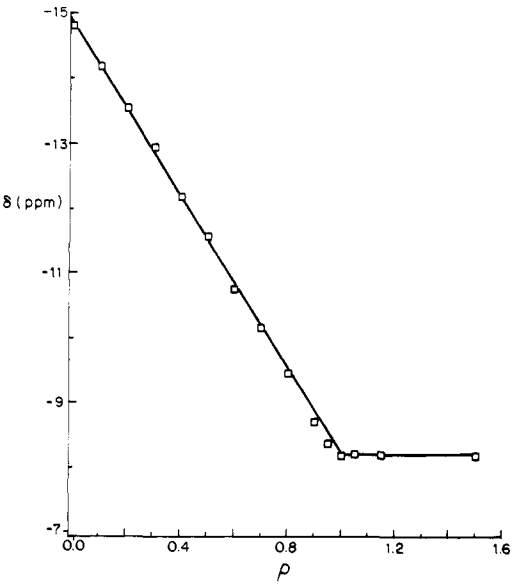

Figure 1. ^{23}Na chemical shifts as a function of the ratio [DB24C8]/[$NaPF_6$] (ρ) in nitromethane. [$NaPF_6$] = 0.037 M.

Experimental Section

Dibenzo-18-crown-6 was synthesized following Pedersen's procedure[1] and recrystallized from ethyl acetate. Dibenzo-24-crown-8 was obtained from Parish Chemical Co. and was recrystallized from ethyl acetate. Sodium tetraphenylborate (Aldrich, 99+%) and the crystalline crown ethers were vacuum-dried (60 °C) over P_2O_5 for at least 16 h prior to use. Sodium tetrafluoroborate (Alfa) was recrystallized from methanol and vacuum-dried for 16 h (70 °C). Sodium hexafluorophosphate (Aldrich, 98.5+%) was recrystallized from acetonitrile and vacuum-dried for 2 days (room temperature). Nitromethane (NM) (Aldrich, 96%, Gold Label), acetonitrile (AN) (Fisher Certified ACS), and dimethylformamide (DMF) (Fisher Certified ACS) were dried, under reflux, over calcium hydride for 3 h, distilled under nitrogen, and stored under argon. DMF was stored over 4-Å molecular sieves. All spectra were recorded within 24 h after the preparation of the samples. NMR tubes were sealed with Parafilm under argon.

^{23}Na NMR spectra were obtained as described previously;[28,29] 90° pulse widths were 22 (79.35 MHz) and 20 μs (52.92 MHz). T_1 measurements were done by using the inversion-recovery 180°–τ–90° pulse sequence and were obtained from a three-parameter nonlinear regression analysis. In the case of Lorentzian line shape, the transverse relaxation rates, T_2^{-1}, were obtained directly from the line width. The temperature in the probe was measured with a thermocouple submerged in a nitromethane or acetonitrile solution in a nonspinning 10-mm NMR tube. The temperature of the sample was estimated to be reliable at ±0.5 K (the measured range of temperature was between 258 and 333 K).

Pseudo-first-order rate constants were obtained from a full line-shape analysis for two-site exchange[30,31] using a Simplex fitting procedure[32] or from the equation derived by Woessner for the case of a moderately rapid exchange.[33]

The chemical shifts were referenced to sodium chloride at infinite dilution in water. They were corrected for the bulk susceptibility differences between the organic solvents and the aqueous reference sample.

Results

The NMR phenomenon is characterized by two different relaxation times. The longitudinal relaxation time, T_1, is essentially energy-driven since the nuclei recover their more stable configuration by dissipation of energy to the lattice. The transverse relaxation time, T_2, is entropy-driven and corresponds to a gradual loss of the phase coherence by exchange of energy between the excited spins. The global energy of the system is not changed in

(6) Wallace, W.; Chen, C.; Eyring, E. M.; Petrucci, S. *J. Phys. Chem.* **1985**, *89*, 1357–1366.
(7) Chen, C.; Wallace, W.; Eyring, E. M.; Petrucci, S. *J. Phys. Chem.* **1984**, *88*, 2541–2547.
(8) Cox, B. G. *Annu. Rep. Prog. Chem.* **1985**, *81(C)*, 43–80.
(9) Detellier, C. In *NMR of Newly Accessible Nuclei*; Laszlo, P., Ed.; Academic: New York, 1983; Vol. 2, Chapter 5, pp 105–151.
(10) Aalmo, K. M.; Krane, J. *Acta Chem. Scand., Ser. A* **1982**, *A36*, 219–225.
(11) Shchori, E.; Jagur-Grodzinski, J.; Luz, Z.; Shporer, J. *J. Am. Chem. Soc.* **1971**, *93*, 7133–7138.
(12) Delville, A.; Stöver, H. D. H.; Detellier, C. *J. Am. Chem. Soc.* **1985**, *107*, 4172–4175.
(13) Strasser, B. P.; Popov, A. I. *J. Am. Chem. Soc.* **1985**, *107*, 7921–7924.
(14) Strasser, B. O.; Hallenga, K.; Popov, A. I. *J. Am. Chem. Soc.* **1985**, *107*, 789–792.
(15) Lin, J. D.; Popov, A. I. *J. Am. Chem. Soc.* **1981**, *103*, 3773–3777.
(16) Shchori, E.; Jagur-Grodzinski, J.; Shporer, M. *J. Am. Chem. Soc.* **1973**, *95*, 3842–3846.
(17) Degani, H. *Biophys. Chem.* **1977**, *6*, 345–349.
(18) Phillips, R. C.; Khazaeli, S.; Dye, J. L. *J. Phys. Chem.* **1985**, *89*, 606–612.
(19) Ceraso, J. M.; Smith, P. B.; Landers, J. S.; Dye, J. L. *J. Phys. Chem.* **1977**, *81*, 760–766.
(20) Ceraso, J. M.; Dye, J. L. *J. Am. Chem. Soc.* **1973**, *95*, 4432–4434.
(21) Bouquant, J.; Delville, A.; Grandjean, J.; Laszlo, P. *J. Am. Chem. Soc.* **1982**, *104*, 686–691.
(22) Schmidt, E.; Popov, A. I. *J. Am. Chem. Soc.* **1983**, *105*, 1873–1878.
(23) Shporer, M.; Luz, Z. *J. Am. Chem. Soc.* **1975**, *97*, 665–666.
(24) Mei, E.; Popov, A. I.; Dye, J. L. *J. Phys. Chem.* **1977**, *81*, 1677–1681.
(25) Mei, E.; Popov, A. I.; Dye, J. L. *J. Am. Chem. Soc.* **1977**, *99*, 6532–6536.
(26) Mei, E.; Dye, J. L.; Popov, A. I. *J. Am. Chem. Soc.* **1977**, *99*, 5308–5311.
(27) Strasser, B. O.; Shamsipur, M.; Popov, A. I. *J. Phys. Chem.* **1985**, *89*, 4822–4824.
(28) Stöver, H. D. H.; Delville, A.; Detellier, C. *J. Am. Chem. Soc.* **1985**, *107*, 4167–4171.
(29) Stöver, H. D. H.; Maurice, L. J.; Delville, A.; Detellier, C. *Polyhedron* **1985**, *4*, 1091–1094.
(30) Sandström, J. *Dynamic NMR Spectroscopy*; Academic: New York, 1982.
(31) Gutowsky, H. S.; Holm, C. H. *J. Chem. Phys.* **1956**, *25*, 1228–1234.
(32) Deming, S. N.; Morgan, S. S. *Anal. Chem.* **1973**, *45A*, 278–282.
(33) Woessner, D. E. *J. Chem. Phys.* **1961**, *35*, 41–48.

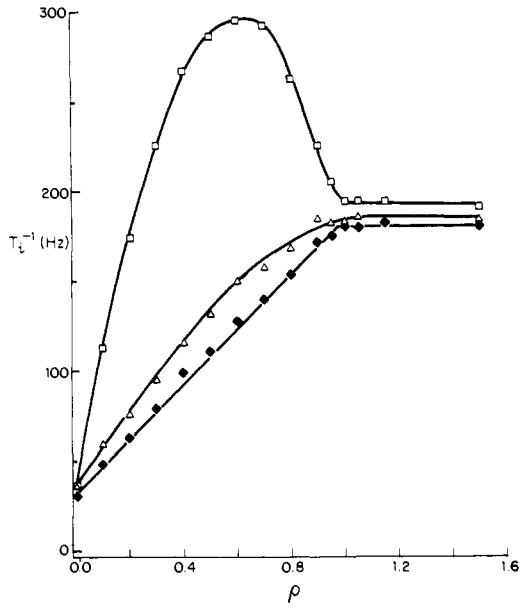

Figure 2. ^{23}Na transverse (i = 2 (△, □)) and longitudinal (i = 1 (♦)) relaxation rates as a function of the ratio [DB24C8]/[$NaPF_6$] (ρ) in nitromethane at 79.35 MHz (□, ♦) and 21.04 MHz (△). The temperatures of measurement were 294 K (□, ♦) and 297 K (△). All line shapes were Lorentzian. [$NaPF_6$] = 0.037 M.

the latter process.[34] From the Bloch equations modified for chemical exchange,[30,31,33] it appears that the crucial difference between T_1 and T_2 lies in the implication of the chemical shift difference in the case of T_2 only. As a result, when the chemical exchange is fast compared to the relaxation rates ($k_{ex} \gg T_2^{-1}$, T_1^{-1}), an information transfer can occur during the transverse relaxation process, and the transverse relaxation rate becomes the composite of relaxation mechanisms and exchange contributions, if the chemical shift difference is large enough. Under these conditions ("moderately rapid exchange"), the chemical exchange process does not affect the longitudinal relaxation time. Consequently, the measurement of both T_1 and T_2 provides the exchange contribution to the transverse relaxation rate[12] and permits the direct calculation of the rate constant in the simple case of a two-site uncoupled system.[33] ^{23}Na NMR is particularly well suited for this purpose since the approach described above requires a rate constant which is large compared to the relaxation rates characteristic of the two sites and in the order of magnitude of the chemical shift difference. The two conditions are fulfilled for rate constants in the order of magnitude of 10^4 s^{-1}.[12] Typical ^{23}Na relaxation rates of solvated sodium are in the range 20 (in water) to 1000 s^{-1} (in a viscous solvent, such as propylene carbonate) and typical relaxation rates of crowned sodium are 200 s^{-1} for Na^+–DB24C8 and 300 s^{-1} for Na^+–DB18C6 in nitromethane. In nitromethane, the chemical shift difference ($\omega_A - \omega_B$) between the two sites, solvated (ω_A) and crowned (ω_B), is 3500 (Na^+–DB24C8) or 1500 rad s^{-1} (Na^+–DB18C6). We have used this approach to study the kinetics of the system $NaBPh_4$–DB24C8 in nitromethane.[12] In this case we found the formation of (n + 1):n aggregates, which we attributed to the propensity of the tetraphenylborate counteranion to assist in the formation of such aggregates.[28]

Dibenzo-24-crown-8. Figure 1 shows the ^{23}Na chemical shift variation of $NaPF_6$ in the presence of increasing amounts of DB24C8 in nitromethane. The linear relationship and the sharp cutoff for a ratio ρ = [DB24C8]/[$NaPF_6$] equal to 1.0 indicate the formation of a complex with a stoichiometry 1:1, characterized by a large complexation constant K_c, for which only a lower limit can be estimated ($K_c \geq 10^5$). If there are only two species in the solution, namely, the solvated and the crowned sodium, a similar behavior is expected for the longitudinal relaxation rate. This

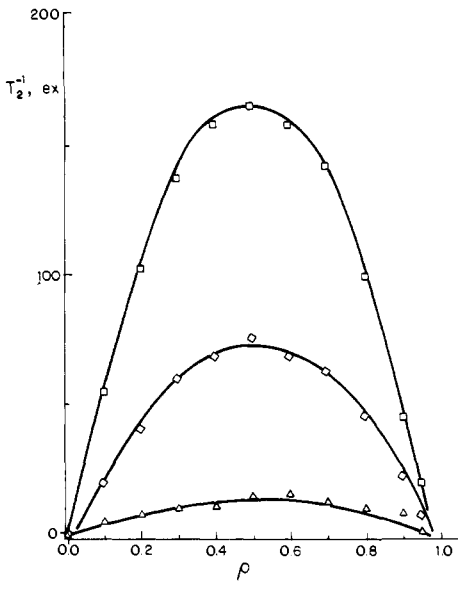

Figure 3. Chemical exchange contribution to the ^{23}Na transverse relaxation rate ($T_{2,ex}^{-1}$) for sodium hexafluorophosphate in the presence of dibenzo-24-crown-8 in nitromethane as a function of ρ = [DB24C8]/[$NaPF_6$]. [$NaPF_6$] = 0.037 M. (□) 79.35 MHz; (◇) 52.92 MHz; (△) 21.04 MHz.

is what is actually observed in Figure 2. There is a linear increase of T_1^{-1} as a function of ρ, from 35 (ρ = 0.0) to 180 Hz (ρ = 1.0). A plateau is observed for $\rho \geq 1.0$. This behavior is different from what we have previously reported for cases involving the tetraphenylborate anion.[28] At the concentration investigated (3.7×10^{-2} M), the hexafluorophosphate anion does not promote aggregation. In Figure 2 are also shown the T_2^{-1} values (obtained directly from the line width of the Lorentzian signal) as a function of ρ for two different field strengths. A maximum is observed for $\rho \sim 0.6$; the measured relaxation rates, $T_{2,obsd}^{-1}$, contain quadrupolar, chemical exchange, and inhomogeneity contributions (eq 1).

$$T_{2,obsd}^{-1} = T_{2,q}^{-1} + T_{2,ex}^{-1} + T_{2,inh}^{-1} \quad (1)$$

In the case of chemical exchange between two uncoupled sites (eq 2), the exchange contribution, $T_{2,ex}^{-1}$, is related to the pseudo-first-order rate constants, k_A and k_B, through eq 3.[33,35]

$$A \underset{k_B}{\overset{k_A}{\rightleftharpoons}} B \quad (2)$$

$$T_{2,ex}^{-1} = 4p_A p_B \pi^2 (\nu_A - \nu_B)^2 (k_A + k_B)^{-1} \quad (3)$$

The curves shown in Figure 3 are in perfect agreement with eq 3, since they are parabolic, displaying a maximum for ρ = 0.5, corresponding to a maximum value of the product $p_A p_B$ (this is expected since $\rho = p_B$ because of the large value of the equilibrium constant of complexation, $K_c \geq 10^5$). Moreover, the relationship with the square of the frequency of observation is fully obeyed: for each ρ value of Figure 3, there is a linear relationship between $T_{2,ex}^{-1}$ and the square of the observation frequency, extrapolating to the origin. The curves in Figure 3 show also the constancy of the sum ($k_A + k_B$) for $0 < \rho < 1.0$. This is a key result, since it opens the way to understanding the mechanism of the complexation–decomplexation process. The unimolecular decomplexation (eq 4) can be ruled out on the basis of the ($k_A + k_B$)

$$Cr + Na^+ \underset{k_{-1}}{\overset{k_1}{\rightleftharpoons}} Cr,Na^+ \quad (4)$$

constancy, since it would lead to eq 5, in which A and B are respectively the sites of solvated and complexed sodium.

$$k_A + k_B = k_1[Cr] + k_{-1} \quad (5)$$

(34) Reisse, J. *NATO ASI Ser., Ser. C* **1983**, *103*, 63–89.

(35) Meiboom, S.; Luz, L.; Gill, D. *J. Chem. Phys.* **1957**, *27*, 1411–1412.

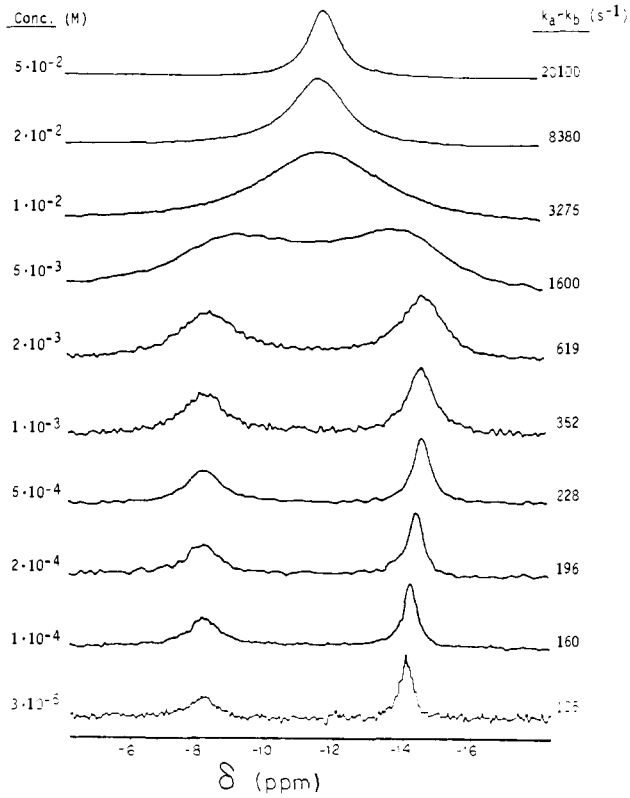

Figure 4. ^{23}Na NMR spectra (79.35 MHz) of sodium hexafluorophosphate solutions in nitromethane in the presence of DB24C8 ($[DB24C8]/[NaPF_6] = 0.50$) at different concentrations (295 K).

In the case of a very high complexation constant, eq 5 becomes eq 6, relating the measured rate constant ($k_A + k_B$) to the ratio ρ.

$$k_A + k_B = k_{-1}(1 - \rho)^{-1} \tag{6}$$

In the hypothesis of a unimolecular decomplexation, ($k_A + k_B$) would depend upon ρ. This is not what is experimentally observed.

A bimolecular cation interchange mechanism (eq 7) leads to apparent rate constants given by eq 8. In this case, the measured

$$Cr,Na^+ + Na^{+*} \overset{k_2}{\rightleftharpoons} Cr,Na^{+*} + Na^+ \tag{7}$$

$$k_A + k_B = k_2[Na^+]_T \tag{8}$$

rate constants are independent of ρ and depend linearly on the total concentration of sodium. Consequently, the mechanism can be further tested: the exchange rate should slow down with dilution of the sample. This is demonstrated in Figure 4. A concentration coalescence is obtained for a total concentration of sodium equal to 5×10^{-3} M.

At this point, it is worth considering a third hypothesis. We have so far neglected the possible role of the anion in the decomplexation process. The extraction of the sodium cation out of the wrapped crown could be assisted by the counteranion as indicated by eq 9 and 10. In this case, the apparent rate constants

$$Na^+ + A^- \overset{K_{IP}}{\rightleftharpoons} Na^+,A^- \tag{9}$$

$$Cr + Na^+,A^- \underset{k_-}{\overset{k_+}{\rightleftharpoons}} Cr,Na^+ + A^- \tag{10}$$

would be given by eq 11, which is equivalent to eq 12 (in the case

$$k_A + k_B = k_+[Cr] + k_-[A^-] \tag{11}$$

$$k_A + k_B = k_-\left(\frac{\rho[Na^+]_T}{[Na^+]K_{IP}} + [A^-]\right) \tag{12}$$

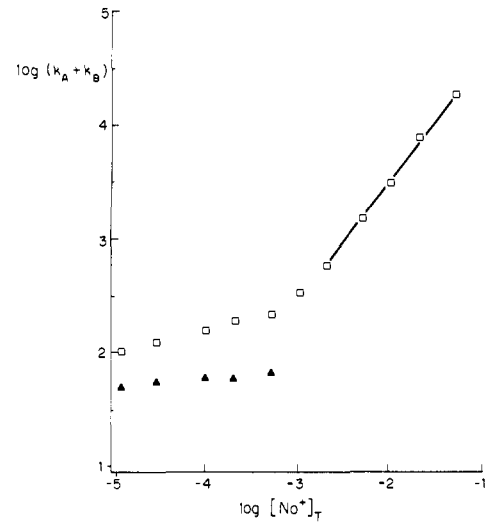

Figure 5. Values of log ($k_A + k_B$) as a function of log $[Na^+]_T$ for $[DB24C8]/[NaPF_6] = 0.50$ in nitromethane. (□) Calculated by full line-shape analysis. The values for $[Na^+]_T > 1.0 \times 10^{-3}$ M were additionally checked by using eq 3. (▲) Residual unimolecular exchange rates obtained by subtracting the extrapolated bimolecular exchange rate contribution from the observed ($k_A + k_B$). (See text.)

of a high complexation constant). For PF_6^-, one can assume that K_{IP} is very small, and, using appropriate approximations, one obtains eq 13. In this case, the measured rate constant should

$$k_A + k_B = k_-[Na^+]_T\frac{\rho}{(1 - \rho)K_{IP}} \tag{13}$$

depend not only upon the total salt concentration but also upon the ρ ratio. If this mechanism were operative, the curves in Figure 2 would definitely not be parabolic.

Figure 5 shows the dependence of ($k_A + k_B$) upon the total sodium concentration for $\rho = 0.5$. At high concentrations (above 2×10^{-3} M) we find the linear variation of ($k_A + k_B$) with $[Na^+]_T$ as predicted for the bimolecular exchange mechanism, with a slope $k_2 = 4.2 \times 10^5$ s^{-1} ($\Delta G^\ddagger = 41$ kJ mol^{-1} at 300 K). Toward the low-concentration limit the bimolecular exchange mechanism becomes less efficient and the exchange rate becomes independent of the total sodium concentration. Thus, for low concentrations, we find a residual unimolecular exchange to be operative. From eq 6, we obtain the value of $k_{-1} = 60$ s^{-1}, corresponding to a free activation energy of 63 kJ mol^{-1} (300 K).

The two values of $\Delta G^\ddagger$ for the two mechanisms are identical with the ones that we have previously determined in the case of the tetraphenylborate anion.

A full line-shape analysis based upon the modified Bloch equations[30] was performed inside a Simplex optimization procedure[32] in order to obtain the exchange rates over the whole concentration range. Additionally, the Lorentzian coalesced signals at concentrations above 10^{-2} M were analyzed via eq 3, yielding identical values for ($k_A + k_B$). The Eyring activation parameters for the bimolecular exchange were $\Delta H^\ddagger = 30 \pm 2$ kJ mol^{-1} and $\Delta S^\ddagger = -37 \pm 10$ J K^{-1} mol^{-1} (from measurements of k_2 at six different temperatures on a solution 0.037 M in $NaPF_6$, with $\rho = 0.5$). These values are, within the error limits, identical with those previously found for the tetraphenylborate counteranion ($\Delta H^\ddagger = 31 \pm 3$ kJ mol^{-1} and $\Delta S^\ddagger = -32 \pm 10$ J K^{-1} mol^{-1}).[23]

Dibenzo-18-crown-6. The structure of the complex crown-Na^+ is different for the two cases of DB24C8 and DB18C6. We have shown previously that, in solution, the DB24C8 wraps around the sodium cation, expelling the solvent molecules and the anion from the first solvation shell.[36] The situation is very different in the case of DB18C6: the crystal structure shows that the cation lies in the center of the crown ring, which is slightly bent, and is

(36) Bisnaire, M.; Detellier, C.; Nadon, D. *Can. J. Chem.* **1982**, *60*, 3071–3076.

coordinated to the anion and/or crystallization water molecules.[37,38] Live and Chan[39] have shown that the structure of the complex in solution is very similar to the one in the crystal. However, in solution, there is a rapid interconversion between the gauche rotamers, while, in the solid state, gauche and trans rotamers have been shown to coexist.[37] If one compared DB18C6 with DB24C8, one would expect a different behavior for the exchange mechanisms. Particularly, a stronger solvent or anion effect could be anticipated in the case of DB18C6. Shchori et al.[11,16] have studied the decomplexation kinetics of Na^+–DB18C6 (at high concentrations, and with a constant ionic strength of about 1 M) in three solvents of similar donicity (dimethylformamide (DMF), DN = 26.6; methanol (MeOH), DN = 25.7; dimethoxyethane (DME), DN = 20.0) with SCN^- (MeOH and DMF) or BPh_4^- (DME) as the counteranions. They found a unimolecular mechanism to be operative for the decomplexation and the Arrhenius energy of activation for that process to be nearly constant (53 kJ mol^{-1}) in the three solvents. In our study, we have avoided the use of strongly ion-pairing anions, such as thiocyanate, and we have worked on dilute solutions (2×10^{-2} M). In DMF, at room temperature, we did not find any exchange contribution to the line shape: the signal was Lorentzian, and T_1 was equal to T_2, within the limits of the homogeneity. A lower detection limit for $(k_A + k_B)$ can be obtained from eq 3: at 300 K, for $\rho = 0.5$, $(k_A + k_B) \geq 2.8 \times 10^4$ s^{-1} (in this estimation, we assume that we could measure $T_{2,ex}^{-1} = T_{2,obsd}^{-1} - T_1^{-1} - T_{2,inh}^{-1}$, if $T_{2,obsd}^{-1} \geq 1.10(T_1^{-1} + T_{2,inh}^{-1})$; in other words, we estimate our accuracy on the $T_{2,ex}^{-1}$ contribution as 10% of $T_{2,q}^{-1} - T_{1,q}^{-1}$). This value is in good agreement with the extrapolations that one can make from the data of Shchori et al.[11] From the variation of the ^{23}Na NMR parameters with the concentration, we have obtained a complexation constant for the formation of the 1:1 complex equal to 450 ± 130 (from the chemical shift variation, error = 2σ) or 440 ± 75 (from the line widths), to be compared with the published value of 600.[11]

The kinetics behavior of the complex Na^+–DB18C6 (counteranions: PF_6^-, BPh_4^-, or BF_4^-) was analyzed in two low-donicity solvents: nitromethane (NM) (DN = 2.7) and acetonitrile (AN) (DN = 14.1), which have comparable dielectric constants (ϵ_{NM} = 35.9, ϵ_{AN} = 38). In the case of $NaBPh_4$ in acetonitrile, a concentration study at a fixed ratio $\rho = 2.0$ led, upon high dilution, to detectable amounts of noncomplexed sodium. This permitted the determination of log $K_f = 5.0 \pm 0.1$.

Parts a and b of Figure 6 show the variations of the ^{23}Na chemical shift of $NaBPh_4$ in acetonitrile as a function of the ratio $\rho = [DB18C6]/[Na^+]$ at two different concentrations. The two curves are very nearly superimposable. An intriguing result is the significant deviation from the straight line expected on the basis of the high equilibrium constant.

The absence of concentration effects excludes the possible contribution of complexes with stoichiometries other than 1:1. We can also rule out the possibility of a specific interaction of the tetraphenylborate anion with the crown phenyl rings, which could affect the diamagnetic part of the ^{23}Na chemical shift, since the same effect is observed for $NaBF_4$. Moreover, the longitudinal relaxation rates display the straight-line behavior expected on the basis of the high equilibrium constant, indicating the presence in solution of only two species, the solvated and the crowned sodium. We should also emphasize that the T_1^{-1} measurements (Figure 6c,d) are a more sensitive probe for the presence of dissymmetric or aggregated species than are the chemical shifts.[28] The T_2^{-1} values are shown in Figure 7. They are very different from the longitudinal relaxation rates and display a maximum at a ratio $\rho \sim 0.4$. They are almost identical in the cases of the two anions studied (BPh_4^- and BF_4^-) and, within the error limits, do not depend upon the concentration of the salt. If this transverse relaxation rate increase was due to an exchange contribution, we can already rule out the bimolecular cation interchange mechanism that we have shown to be the dominant mechanism in the case of DB24C8. A careful examination of the signal line shape indicates, for $\rho < 0.4$, that the signal is not truly Lorentzian. This can be attributed to the beginning of a coalescence. As shown by eq 6, which is given for the case of a unimolecular decom-

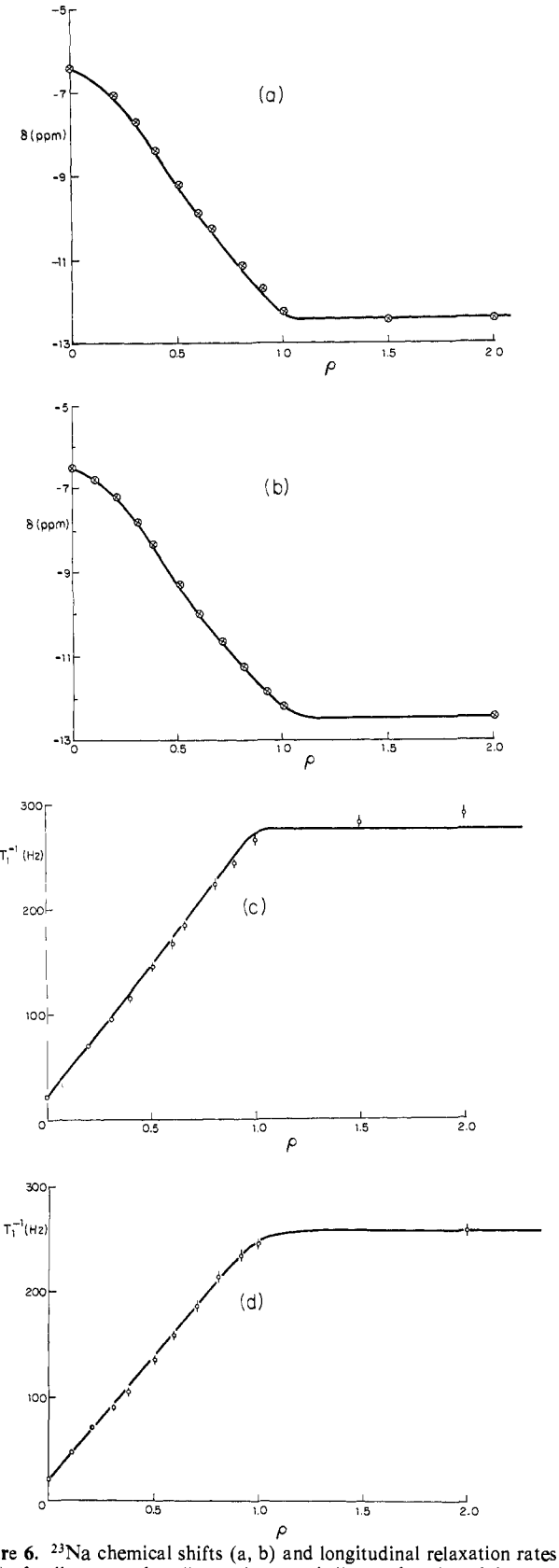

Figure 6. ^{23}Na chemical shifts (a, b) and longitudinal relaxation rates (c, d) of sodium tetraphenylborate in acetonitrile as a function of the ratio [DB18C6]/[Na^+]. (a, c) [$NaBPh_4$] = 2.0×10^{-2} M; (b, d) [$NaBPh_4$] = 5.0×10^{-3} M. The data points are experimental and the curves are calculated with values of $k_{-1} = 2600 \pm 100$ s^{-1}. (See text.)

(37) Bright, D.; Truter, M. R. *J. Chem. Soc. B* **1970**, 1544–1550.
(38) Bush, M. A.; Truter, M. R. *J. Chem. Soc. B* **1971**, 1440–1446.
(39) Live, D.; Chan, S. I. *J. Am. Chem. Soc.* **1976**, *98*, 3769–3778.

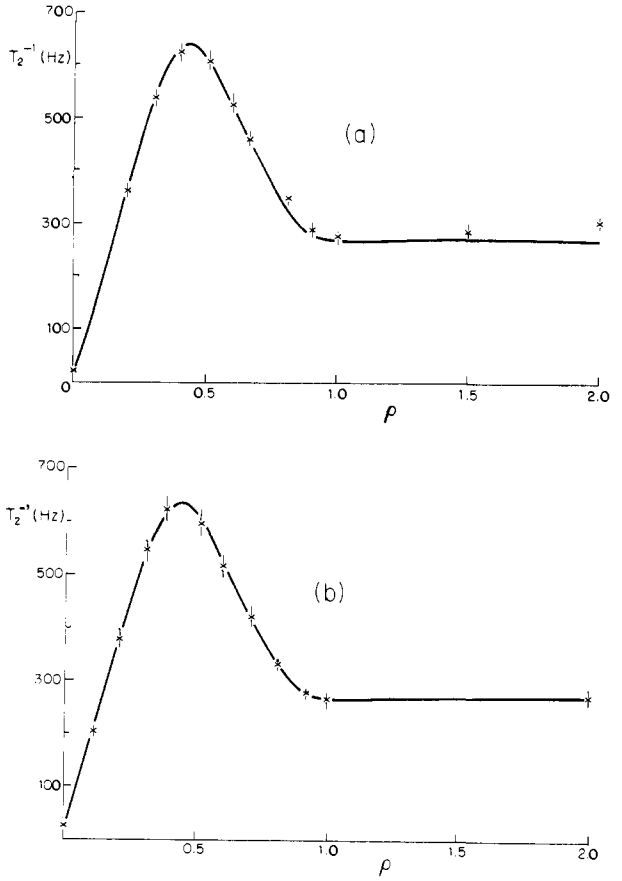

Figure 7. ^{23}Na transverse relaxation rates of sodium tetraphenylborate in acetonitrile as a function of the ratio [DB18C6]/[Na^+]. (a) [$NaBPh_4$] = 2.0×10^{-2} M; (b) [$NaBPh_4$] = 5.0×10^{-3} M. The data points are experimental and the curves are calculated with values of $k_{-1} = 2600 \pm 100$ s^{-1}.

plexation mechanism, this is indeed what is expected, since the observed rate constant $(k_A + k_B)$ is linearly related to $(1 - \rho)^{-1}$. Using the classical equations for an uncoupled two-site exchange[30] we were able to simulate the line shape in order to obtain apparent chemical shifts and transverse relaxation rates. This is shown in Figures 6 and 7, in which all data points are experimental and the curves have been calculated from a k_{-1} rate constant. We have also calculated the longitudinal relaxation rate expected from the rate constant obtained from the line-shape analysis. In order to achieve it, we have used full treatment of the longitudinal relaxation matrix including exchange contributions.[33] Again, on Figure 6, the T_1 data points are experimental, and the curve is calculated. So, all three observables (chemical shifts and transverse and longitudinal relaxation rates) are in perfect agreement with the unimolecular decomplexation mechanism. For five temperatures, we have performed a full line-shape analysis at three different values of ρ. The agreement with a pure unimolecular decomplexation mechanism is excellent as shown on Figure 8. The relationship between the measured rate constants, $(k_A + k_B)$, and $(1 - \rho)^{-1}$ (eq 6) is perfectly linear, extrapolating to the origin. The slope of each straight line gives k_{-1}. The Eyring plot is shown on Figure 9 and gives the activation parameters $\Delta H^{\ddagger} = 40 \pm 2$ kJ mol^{-1} and $\Delta S^{\ddagger} = -44 \pm 8$ J mol^{-1} K^{-1} ($\Delta G^{\ddagger}_{300} = 53 \pm 2$ kJ mol^{-1}).

The spectra were very different in nitromethane: two well-separated resonances were observed for $NaPF_6$ in the presence of DB18C6. A full line-shape analysis[30] was again performed on these spectra. The measured rates $(k_A + k_B)$ are given as a function of $(1 - \rho)^{-1}$ for $NaPF_6$ (Figure 10a) and $NaBPh_4$ (Figure 10b) at different concentrations. As for the case of acetonitrile the relationships are linear, showing a unimolecular decomplexation mechanism to be operative. *However*, in this case, there is an important difference: the straight lines *do not* extrapolate

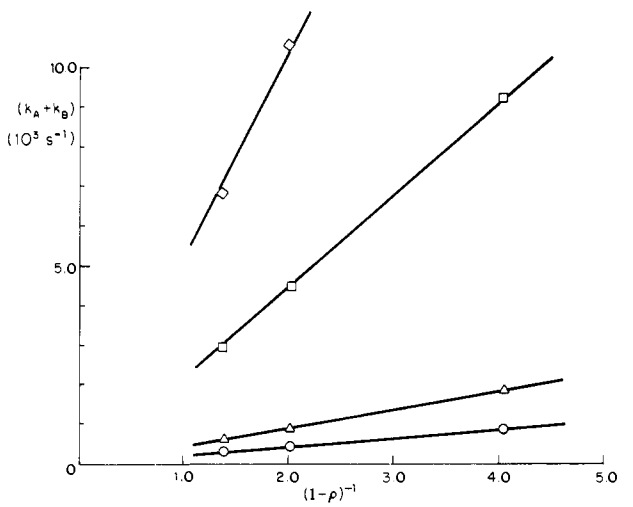

Figure 8. $(k_A + k_B)$ as a function of $(1 - \rho)^{-1}$ for various temperatures in acetonitrile. [$NaBPh_4$] = 1.0×10^{-2} M. (○) 258 K, $k_{-1} = (2.3 \pm 0.1) \times 10^2$ s^{-1}; (△) 268 K, $k_{-1} = (4.5 \pm 0.1) \times 10^2$ s^{-1}; (□) 294 K, $k_{-1} = (2.2 \pm 0.1) \times 10^3$ s^{-1}; (◇) 308 K, $k_{-1} = (5.2 \pm 0.2) \times 10^3$ s^{-1}. A third data point at 308 K ($(1 - \rho)^{-1} = 4.05$) is not reported on the graph. The data at 322 K have not been reported on the graph: $k_{-1} = (1.1 \pm 0.1) \times 10^4$ s^{-1}. The five linear relationships extrapolate to the origin (eq 6).

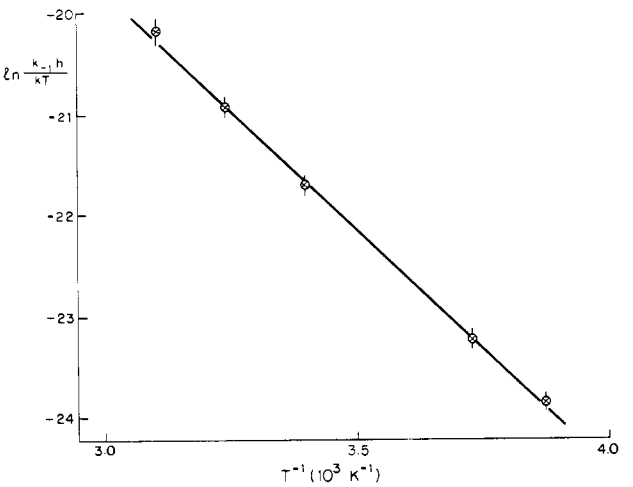

Figure 9. $(\ln k_{-1} - \ln [kT/h])$ as a function of T^{-1}. [$NaBPh_4$] = 1.0×10^{-2} M in acetonitrile. k_{-1} has been obtained from the slopes of the linear relationships between $(k_A + k_B)$ and $(1 - \rho)^{-1}$ (eq 6) as shown in Figure 8. Under these conditions, the mechanism is purely unimolecular. Activation parameters: $\Delta H^{\ddagger} = 40 \pm 2$ kJ mol^{-1}; $\Delta S^{\ddagger} = -44 \pm 8$ J mol^{-1} K^{-1}.

to the origin. We can attribute the residual rate constants to a bimolecular mechanism, since they are linearly dependent upon the total sodium concentration. The extrapolated values of the measured $(k_A + k_B)$ obtained from the relationships of Figure 10 are linearly related to $[Na^+]_T$, with an *extrapolation to the origin*. These rate constants $(k_A + k_B)$ can be separated into two contributions, coming respectively from a unimolecular decomplexation mechanism (this contribution depends *only* upon $(1 - \rho)^{-1}$ and gives k_{-1} (eq 6)) and from a bimolecular, cation interchange mechanism (this contribution depends *only* upon $[Na^+]_T$ and gives k_2 (eq 8)). We can rule out any other mechanisms involving, for example, the counteranion, because such mechanisms would imply an interdependency of $(1 - \rho)^{-1}$ and $[Na^+]_T$ (see eq 12 and 13). A set of straight lines similar to the ones previously shown for acetonitrile on Figure 8 are shown on Figure 11. The important difference between Figure 8 and Figure 11 is the extrapolation to residual rate constants in the latter case.

Discussion

Two different mechanisms for the exchange of a cation complexed by a crown ether ligand are observed: a unimolecular

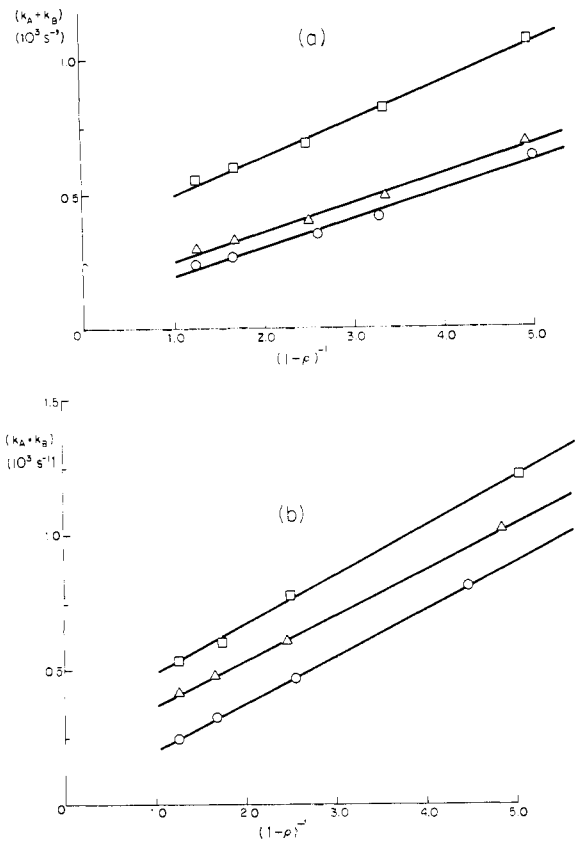

Figure 10. ($K_A + k_B$) as a function of $(1 - \rho)^{-1}$ in nitromethane. T = 294 K. The slopes of the linear relationships give k_{-1} (eq 6). This extrapolation shows a residual bimolecular mechanism and gives k_2-$[Na^+]_T$ (eq 8). (a) PF_6^-: (○) $[Na^+]_T = 5.0 \times 10^{-3}$ M, $k_{-1} = (1.0 \pm 0.1) \times 10^2\ s^{-1}$, $k_2 = (1.7 \pm 0.2) \times 10^4\ s^{-1}\ M^{-1}$; (△) $[Na^+]_T = 8.5 \times 10^{-3}$ M, $k_{-1} = (1.0 \pm 0.1) \times 10^2\ s^{-1}$, $k_2 = (1.7 \pm 0.3) \times 10^4\ s^{-1}\ M^{-1}$; (□) $[Na^+]_T = 2.1 \times 10^{-2}$ M, $k_{-1} = (1.3 \pm 0.1) \times 10^2\ s^{-1}$, $k_2 = (1.7 \pm 0.2) \times 10^4\ s^{-1}\ M^{-1}$. (b) BPh_4^-: (○) $[Na^+]_T = 4.2 \times 10^{-3}$ M, $k_{-1} = (1.7 \pm 0.1) \times 10^2\ s^{-1}$, $k_2 = (0.6 \pm 0.4) \times 10^4\ s^{-1}\ M^{-1}$; (△) $[Na^+]_T = 8.8 \times 10^{-3}$ M, $k_{-1} = (1.7 \pm 0.1) \times 10^2\ s^{-1}$, $k_2 = (2.3 \pm 0.3) \times 10^4\ s^{-1}\ M^{-1}$; (□) $[Na^+]_T = 2.0 \times 10^{-2}$ M, $k_{-1} = (1.8 \pm 0.1) \times 10^2\ s^{-1}$, $k_2 = (1.5 \pm 0.2) \times 10^4\ s^{-1}\ M^{-1}$.

decomplexation mechanism when Na^+ is complexed by DB18C6 in acetonitrile and a competition between bimolecular cation exchange and unimolecular decomplexation mechanisms when Na^+ is complexed by DB24C8 or DB18C6 in nitromethane. In this case, a concentration study permits the differentiation of the two mechanistic contributions to the observed rate constants. Also, we can rule out any mechanism in which the anion, involved in the transition state, would assist the decomplexation process. This statement is true for the cases of the tetraphenylborate, tetrafluoroborate, and hexafluorophosphate anions in nitromethane or acetonitrile. We will discuss elsewhere the cases of the thiocyanate and the iodide anions.[40]

Table I gives the activation parameters of decomplexation for Na^+-DB18C6 complexes in some solvents. The dissociative exchange is slower in low-donicity solvents: the free energy of activation increases steadily from 45 kJ mol^{-1} in DMF (DN = 26.6) to 60 kJ mol^{-1} in nitromethane (DN = 2.7). This increase results from the compensation of the decrease in activation enthalpy by the concurrent decrease of the activation entropy, which is positive in DMF ($\Delta S^\ddagger = +21$ J mol^{-1} K^{-1})[11] and largely negative in NM ($\Delta S^\ddagger = -78$ J mol^{-1} K^{-1}).

This trend is reminiscent of what has been shown to be operative in the thermodynamic process of the complexation of cations with crown ethers, cryptands, glymes, podands, or antibiotics.[41] This compensation effect of ΔH and ΔS had previously been pointed out by Michaux and Reisse[42] and Izatt et al.[43] It is interesting

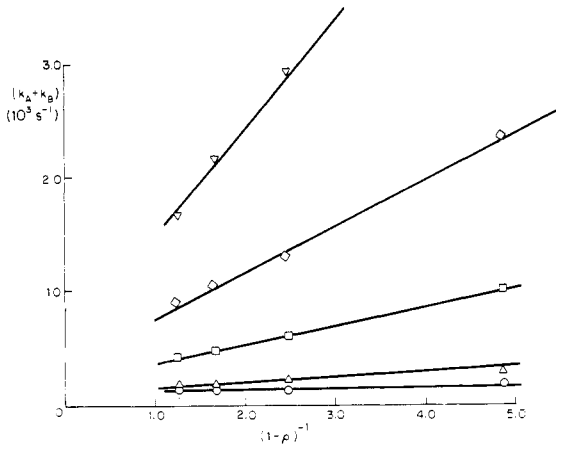

Figure 11. ($k_A + k_B$) as a function of $(1 - \rho)^{-1}$ for various temperatures in nitromethane. $[NaBPh_4] = 8.8 \times 10^{-3}$ M. (○) 259 K, $k_{-1} = (1.2 \pm 0.9) \times 10^1\ s^{-1}$, $k_2 = (1.3 \pm 0.6) \times 10^4\ s^{-1}\ M^{-1}$; (△) 271 K, $k_{-1} = (5.0 \pm 0.6) \times 10^1\ s^{-1}$, $k_2 = (1.1 \pm 0.3) \times 10^4\ s^{-1}\ M^{-1}$; (□) 294 K, $k_{-1} = (1.7 \pm 0.1) \times 10^2\ s^{-1}$, $k_2 = (2.3 \pm 0.4) \times 10^4\ s^{-1}\ M^{-1}$; (◇) 313 K, $k_{-1} = (4.1 \pm 0.4) \times 10^2\ s^{-1}$, $k_2 = (4 \pm 1) \times 10^4\ s^{-1}\ M^{-1}$; (▽) 331 K, $k_{-1} = (9.4 \pm 0.5) \times 10^2\ s^{-1}$, $k_2 = (6 \pm 2) \times 10^4\ s^{-1}\ M^{-1}$. The five linear relationships do not extrapolate to the origin, showing the presence of a residual bimolecular mechanism (eq 6 and 8). The Eyring activation parameters for k_{-1} are $\Delta H^\ddagger = 37 \pm 3$ kJ mol^{-1} and $\Delta S^\ddagger = -78 \pm 8$ J mol^{-1} K^{-1}. The large errors associated with the determination of k_2 preclude any reliable calculation of the activation parameters for the bimolecular mechanism.

Table I. Activation Parameters for the Decomplexation of Na^+-DB18C6 and Na^+-DB24C8 in Several Solvents[a]

solvent[a]	anion	$\Delta H^\ddagger$, kJ mol^{-1}	$\Delta S^\ddagger$, J mol^{-1} K^{-1}	$\Delta G^\ddagger_{300}$, kJ mol^{-1}	mechanism[g]
		Dibenzo-18-crown-6			
DMF[b]	SCN^-	51	+21	45	uni
DME[b]	SCN^-	53	+12	50	uni
MeOH[b]	SCN^-	47	−10	50	uni
AN[c]	BF_4^-	40 ± 2	−44 ± 8	53 ± 2	uni
AN[c]	BPh_4^-	40 ± 2	−44 ± 8	53 ± 2	uni
NM[c]	BPh_4^-	37 ± 3	−78 ± 8	60 ± 3	uni
NM[c]	BPh_4^-	nd[e,f]	nd[f]	48 ± 4	bi
NM[c]	PF_6^-	nd	nd	60 ± 3	uni
NM[c]	PF_6^-	nd	nd	47 ± 3	bi
		Dibenzo-24-crown-8			
NM[c]	PF_6^-	30 ± 2	−37 ± 10	40 ± 2	bi
NM[c]	PF_6^-	nd	nd	~63	uni
NM[d]	BPh_4^-	31 ± 3	−32 ± 10	41 ± 3	bi
NM[d]	BPh_4^-	nd	nd	~65	uni

[a] DMF = dimethylformamide, DME = dimethoxyethane, MeOH = methanol, AN = acetonitrile, NM = nitromethane. [b] Reference 11. [c] This work. [d] Reference 12. [e] nd = not determined. [f] In this case, a temperature study has been done (see Figure 11). $\Delta H^\ddagger$ and $\Delta S^\ddagger$ could be determined from the values of ($k_A + k_B$) extrapolated at $(1 - \rho)^{-1} = 0$. However, the uncertainties associated with that extrapolation preclude any useful determination of the activation parameters. [g] uni = unimolecular decomplexation (eq 4); bi = bimolecular cation interchange (eq 7).

to see the same phenomenon applying to the kinetic parameters of the decomplexation process. The origin of the compensation effect in the case of the thermodynamic parameters can be attributed to a variety of causes.[41] Therefore, it would be oversimplistic to try to attribute the observed trend of the kinetic parameters to a single cause. Moreover, we have only a limited amount of data. It has been shown that a statistical compensation pattern arising from experimental errors can be the major cause of the dependence between ΔH and ΔS.[44] The relationship

(40) Stöver, H. D. H.; Detellier, C., to be published.
(41) Inoue, Y.; Hakushi, T. *J. Chem. Soc., Perkin Trans. 2* **1985**, 935–946.
(42) Michaux, G.; Reisse, J. *J. Am. Chem. Soc.* **1982**, *104*, 6895–6899.
(43) Izatt, R. M.; Terry, R. E.; Haymore, B. L.; Hansen, L. D.; Dalley, N. K.; Avondet, A. G.; Christensen, J. J. *J. Am. Chem. Soc.* **1976**, *98*, 7620–7626.

Scheme I. Speculative Scenario of the Na^+–DB18C6 Complexation/Decomplexation Processes[a]

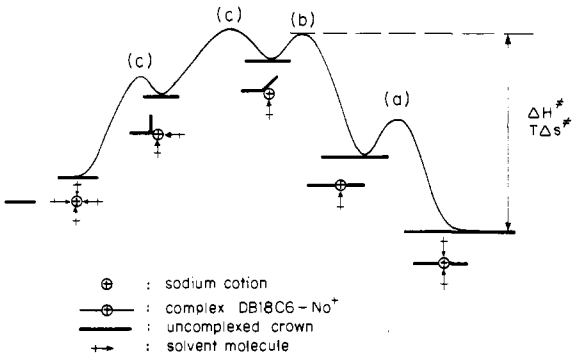

[a] (a) Desolvation. The loss of one solvent molecule is accompanied by solvent cage reorganization. (b) Conformational change of the ligand, with loss of coordination and solvent cage reorganization. Steps a and b could be concerted. (c) Loss of more coordination sites. Entry of solvent molecules.

between $\Delta G^{\ddagger}$ at 300 K (close to the harmonic mean of the experimental temperatures) and $\Delta H^{\ddagger}$ shows also a qualitative trend: $\Delta G^{\ddagger}$ increases from DMF to NM when $\Delta H^{\ddagger}$ decreases. This is a good indication that the cause of the $\Delta H^{\ddagger}$–$\Delta S^{\ddagger}$ relationship has a chemical origin.[45]

What is the nature of the transition state for the unimolecular decomplexation of the Na^+–DB18C6 complex? If one or more solvent molecules were replacing one or more crown ether oxygens in the process leading to the activated complex, one would expect $\Delta H^{\ddagger}$ in DMF to be lower than in NM, since the enthalpy cost for the replacement of ether oxygen donor atoms by a solvent molecule would be lower in the better coordinating DMF solvent than in NM, whose donicity number is only 2.7. The opposite trend is observed: $\Delta H^{\ddagger}_{NM} < \Delta H^{\ddagger}_{DMF}$.

The crystal structure of Na^+–DB18C16 resembles a slightly bent receptacle in which lies the cation, coordinated to two water molecules and/or the counteranion.[37,38] Live and Chan[39] have shown that the ligand structure is the same in the solution (chloroform and acetone) as in the crystal and we have evidence for the participation of more than one (plausibly two) solvent molecule in the coordination sphere of the crowned sodium in dimethylformamide, acetonitrile, pyridine, and nitromethane.[46] If we consider that, in the investigated solvents, the complexed sodium cation is coordinated to all six ether oxygens and to two solvent molecules, any hypothesis based on the *stepwise* replacement of ether donor atoms by solvent molecules suffers from a major drawback: how could the crown ether leave the sodium environment in which it is "locked" by the two solvent molecules on each side of the quasi-planar conformation?

We can envisage the replacement of the oxygen donor atoms by the solvent molecules to go through the following stages (Scheme I): (a) Two or more oxygens *and* one of the two solvent molecules are removed stepwise, *without* a concomitant total replacement by the solvent molecules in the first cationic coordination shell. However, this removal is accompanied by a reorganization of the solvent cage around the complex.

This is the slow part of the process, which we measure in the ^{23}Na NMR experiment. (b) The activated complex may be assumed to be partially decomplexed and desolvated sodium. (c) The stepwise decomplexation following steps a and b is assisted by the concerted approach of solvent molecules to lead to a four-coordinated sodium cation, the plausible sodium coordination number in nonaqueous solutions.[47,48]

The departure of the crown has to follow a partial *desolvation* of the crowned sodium. This desolvation step is reflected in the trend of $\Delta H^{\ddagger}$ and $T\Delta S^{\ddagger}$ going from DMF to NM. A higher $\Delta H^{\ddagger}$ and also a positive contribution of $T\Delta S^{\ddagger}$ are characteristic of the solvent with the highest donicity. This is in keeping with the likely interpretation of the enthalpy–entropy compensation effect: "as the cation–ligand binding becomes stronger, the degree of freedom of the complex is inevitably reduced, owing to increased rigidity of structure".[41] The gain of entropy corresponding to the release of one solvent molecule is compensated by the loss of entropy due to the reorganization of the solvent cage.

The solvent-separated (loose) ion pair possibly formed between the counteranion and the crowned sodium cation could be perturbed during the decomplexation–desolvation process. We have shown that tetraphenylborate and tetrafluoroborate give the same activation parameters in acetonitrile. The use of thiocyanate, a coordinating anion, could have played a role in the work of Shchori et al.,[11,16] at least in the case of dimethoxyethane, a low dielectric constant solvent.

What we measure in ^{23}Na exchange NMR is the difference between the energy state of the complexed sodium and the highest energy state of the decomplexation path. A priori, we have no evidence that the highest energy activated complexes have a similar structure in the different solvents. The proposed decomplexation scenario (Scheme I) is based on the assumption that a similar structure is found in all the investigated solvents, namely, the 8-coordinated sodium cation (6 ether oxygens + 2 solvent molecules), and that the mechanisms of decomplexation are comparable. The steady variation of the activation parameters with the solvent donicity number is a good indication of the similarity of the mechanisms of decomplexation in the various solvents.

The comparison of the results published by Strasser and Popov[13] and Shchori et al.[11,16] on the activation parameters of the decomplexation of NaSCN with 18C6, DC18C6, or DB18C6 in methanol shows a similar entropy–enthalpy compensation, with $\Delta H^{\ddagger}$ increasing from DC18C6 to 18C6 to DB18C6 and $\Delta S^{\ddagger}$ increasing in the same order. This trend is in agreement with our hypothesis involving desolvation and conformational changes in the path to the activated complex. The more rigid DB18C6 has the highest $\Delta H^{\ddagger}$. It is not obvious that the structure of Na^+–18C6 in solution is similar to the one of Na^+–DB18C6. In the solid state, the Na^+–18C6 complex has not the same structure as the Na^+–DB18C6 complex. One of the ether oxygens is displaced by 1.95 Å from the principal plane defined by the five other oxygens. This corresponds to a pentagonal-pyramidal coordination.[49] The difference in the complex structure could lead to a different path in the decomplexation process of 18C6, which could make difficult the comparison with dicyclohexyl-18-crown-6 (DC18C6) and DB18C6. Along that line, it is surprising to find that the values for $\Delta H^{\ddagger}$ and $\Delta S^{\ddagger}$ of the decomplexation of Na^+–18C6 lie between those for Na^+–DB18C6 and Na^+–DC18C6.[13]

The postulate by Shchori et al.[11,16] that the major barrier to dissociation for these complexes is conformational in origin did not recognize the role of the solvent. The data for solvents with much lower donicities (acetonitrile and nitromethane) than the ones they investigated (dimethylformamide, dimethoxyethane, methanol) show that, in addition to the ligand conformational change, a *desolvation* step should be taken into account.

A few more points have to be discussed regarding the results given in Table I. These results are independent of the nature of the associated counteranion, BPh_4^- or PF_6^-, which are known to be noncoordinating species. In the case of DB18C6 no aggregation induced by BPh_4^- could be detected. This was expected on the basis of our proposal for the structure of aggregated structures in the case of DB24C8,[28] in which the crown adopts a conformation similar to the one found for a 2:1 complex in the solid state.[50]

(44) Krug, R. R.; Hunter, W. G.; Grieger, R. A. *J. Phys. Chem.* **1976**, *80*, 2335–2341.
(45) Krug, R. R.; Hunter, W. G.; Grieger, R. A. *J. Phys. Chem.* **1976**, *80*, 2341–2351.
(46) Lafleur, D. M.; Delville, A.; Maurice, L. J.; Detellier, C., to be published.
(47) Delville, A.; Detellier, C.; Gerstmans, A.; Laszlo, P. *J. Am. Chem. Soc.* **1980**, *102*, 6558–6559.
(48) Delville, A.; Detellier, C.; Gerstmans, A.; Laszlo, P. *Helv. Chim. Acta* **1981**, *64*, 547–555.
(49) Dunitz, J. D.; Dobler, M.; Seiler, P.; Philac Kerley, R. P. *Acta Crystallogr., Sect. B: Struct. Crystallogr. Cryst. Chem.* **1974**, *30B*, 2733–2738.

Scheme II. Scenario of the Bimolecular Cation-Exchange Mechanism of the Na^+-DB24C8 Complex[a]

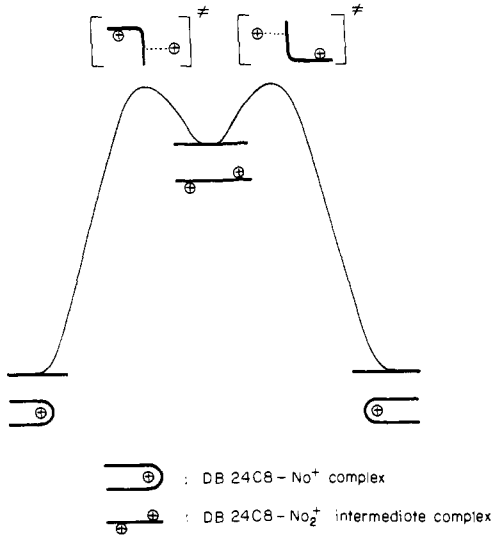

[a] The opening of the wrapped crown is assisted by the approach of a second sodium cation.

Such a conformation is less probable for DB18C6. The reason a bimolecular mechanism does become competitive in nitromethane in the case of DB18C6 lies in the high free energy of activation (60 kJ mol^{-1} at 300 K) of the unimolecular decomplexation process. For nitromethane, coordinating less strongly to sodium than solvents with higher donicities, the gain of translational entropy in the desolvation step (enthalpically more favored) does not compensate for the loss of entropy accompanying the solvent cage reorganization. Consequently, even if the bimolecular process is plausibly entropically disfavored in comparison to the unimolecular process, the additional stabilization afforded by the incoming second sodium cation makes the bimolecular mechanism operative at high enough sodium concentrations.

The activation parameters of the decomplexation of $NaPF_6$-DB24C8 are $\Delta H^{\ddagger}$ = 30 kJ mol^{-1} and $\Delta S^{\ddagger}$ = -37 J mol^{-1} K^{-1} (see Scheme II). These values are identical with those determined previously in the case of the counteranion BPh_4^-.[12] They confirm that the extra stabilization afforded by the second cation is $\Delta G^{\ddagger}$ ~20-25 kJ mol^{-1}. It is particularly interesting to point out that, in nitromethane, a poorly coordinating solvent, $\Delta G^{\ddagger}_{uni}$ is identical in the two cases studied (DB18C6 and DB24C8). In nitromethane, the unimolecular decomplexation barrier results mainly from conformational changes of the ligand. In the case of DB24C8, more oxygen ethers are available to the cation, and accordingly the bimolecular mechanism is favored both for entropy and enthalpy reasons.

In conclusion, this study has demonstrated that a bimolecular decomplexation mechanism has to be expected in poorly coordinating solvents, even in the case of crown ethers too small to wrap around the cation.

Acknowledgment. The Natural Science and Engineering Research Council of Canada (NSERCC) is gratefully acknowledged for financial support. We thank Francine Marleau (NSERCC summer student, 1986) for her help in the computer analysis of some spectra.

Registry No. Na^+-DB24C8·PF_6^-, 110698-01-6; Na^+-DB18C6·PF_6^-, 39019-64-2; Na^+-DB18C6·BPh_4^-, 39152-87-9; Na^+-DB18C6·BF_4^-, 93581-87-4.

(50) Hughes, D. L. *J. Chem. Soc., Dalton Trans.* **1975**, 2374-2378.

Investigation of the Hydration of Zeolite NaA by Two-Dimensional ^{23}Na Nutation NMR

G. A. H. Tijink, R. Janssen, and W. S. Veeman*

Contribution from the Department of Molecular Spectroscopy, Faculty of Science, University of Nijmegen, Toernooiveld, 6525 ED Nijmegen, The Netherlands. *Received February 20, 1987*

Abstract: A two-dimensional nutation NMR experiment is used to observe the change of quadrupole parameters of sodium ions in zeolite NaA when the zeolite is loaded in steps with water. We can detect two sodium sites in the dry zeolite, at respectively 6-rings and 8-rings, and can follow the water absorption at these sites. When the amount of absorbed water is increased in steps, first the quadrupole interaction of sodium at the 6-rings decreases; with more absorbed water the quadrupole interaction of the sodium ions at the 8-rings becomes small. Relaxation effects in the rotating frame, studied by combining rotary echoes with nutation NMR, indicate a mobility of sodium ions or water molecules.

Zeolites are crystalline aluminosilicates consisting of a framework of AlO_4 and SiO_4 tetrahedra which build up a network of channels and cavities.[1] In these micropores there are so-called nonframework cations which balance the negatively charged framework. Zeolites are used in the fields of catalysis, molecular sieves, ion exchange, and medicine.[2-4] For many of these applications the knowledge of the local environment, mobility, and absorptive behavior of the cations is very important; for example, molecular sieving is often controlled by the location and size of these cations.[5,6]

The investigation of these cations has involved a number of techniques,[7-11] of which nuclear magnetic resonance seems to be

(1) Meier, W. M.; Olson, D. H. *Atlas of Zeolite Structure Types*; Structure Commission of the International Zeolite Association, 1978.
(2) Barrer, R. M. *Zeolites and Clay Minerals as Sorbents and Molecular Sieves*; Academic: New York, 1978.
(3) Rabo, J. A. *Catalysis by Zeolites*; Elsevier: Amsterdam, 1980.
(4) Ishibashi, M.; Yoshioko, S.; Monma, J.; Suzuki, Y.; Uchiyama, M.; Watanabe, T.; Takai, S. *Chem. Pharm. Bull.* **1986**, *34*, 2973-2978.
(5) Ruthven, D. M. *Can. J. Chem.* **1974**, *52*, 3523-3528.
(6) Breck, D. W.; Eversole, W. G.; Milton, R. M.; Reed, T. B.; Thomas, T. L. *J. Am. Chem. Soc.* **1956**, *78*, 5972-5977.
(7) Morris, B. J. *Phys. Chem. Solids* **1969**, *30*, 103-115.
(8) Lohse, U.; Stach, H.; Hollnagel, M.; Schirmer, W. *Z. Phys. Chem. (Leipzig)* **1971**, *247*, 65-77.
(9) Stamires, D. N. *J. Chem. Phys.* **1962**, *36*, 3174-3181.
(10) Lechert, H.; Henneke, H. W. *ACS Symp. Ser.* **1977**, *No. 40*, 53-63.
(11) Kunath, D.; Spangenberg, H. J.; Stach, H.; Schirmer, W. *Z. Chem.* **1970**, *1*, 1-9.

0002-7863/87/1509-7301$01.50/0